Early Pliocene climatic optimum, cooling and early glaciation deduced by terrestrial and marine environmental changes in SW Spain

Gonzalo Jiménez-Moreno[1,*], José N. Pérez-Asensio[2], Juan C. Larrasoaña[3,4], Francisco J. Sierro[5], Daniel Garcia-Castellanos[4], Ángel Salazar[6], Josep Maria Salvany[7], Santiago Ledesma[8], M. Pilar Mata[6] and Carlos Mediavilla[9]

[1]*Departamento de Estratigrafía y Paleontología, Universidad de Granada, 18002 Granada, Spain*

[2]*GRC Geociències Marines, Departament de Dinàmica de la Terra i de l'Oceà, Universitat de Barcelona, 08028 Barcelona, Spain*

[3]*Instituto Geológico y Minero de España, Unidad de Zaragoza, 50006 Zaragoza, Spain*

[4]*Institute of Earth Sciences Jaume Almera, Consejo Superior de Investigaciones Científicas, 08028 Barcelona, Spain*

[5]*Department of Geology, University of Salamanca, 37008 Salamanca, Spain*

[6]*Instituto Geológico y Minero de España, 28760 Tres Cantos, Madrid, Spain*

[7]*Departament d'Enginyeria Civil i Ambiental, Universitat Politècnica de Catalunya, 08034 Barcelona, Spain*

[8] *Naturgy Energy Group, S.A., 28033 Madrid, Spain*

[9]*Instituto Geológico y Minero de España, 41013 Sevilla, Spain*

*Corresponding author: Tel: +34 958 248727.
E-mail address: gonzaloj@ugr.es (G. Jiménez-Moreno).

Keywords: pollen analysis, vegetation, benthic foraminifera, climate change, early Pliocene, SW Spain.

Abstract

The Pliocene is a key period in Earth's climate evolution, as it records the transition from warm and stable conditions to the colder and more variable glaciated climate of the Pleistocene. Simultaneously, climate became more seasonal in the Mediterranean area, and Mediterranean-type seasonal precipitation rhythm with summer drought established. These climatic changes presumably had significant impacts on terrestrial environments. However, the response of terrestrial environments to such climate changes is still not fully understood due to the lack of detailed studies dealing with this period of time. In this study, multiproxy analyses of continuous core sampling from La Matilla (SW Spain) shows detailed and continuous record of pollen, sand content and abundance of benthic foraminifer *Bolivina spathulata* to describe paleoenvironmental and paleoclimate trends during the early Pliocene. This record shows warmest, most humid climate conditions and highest riverine nutrient supply at ~ 4.35 Ma, coinciding with the Pliocene climatic optimum and high global sea level. A climate cooling and aridity trend occurred subsequently and a significant glaciation occurred at ~ 4.1-4.0 Ma, during a period known by very little terrestrial evidence of glaciation. Our multiproxy data thus indicate that terrestrial and marine environments were significantly variable during the early Pliocene and that major glaciation-like cooling occurred before the intensification of northern

hemisphere glaciation at the beginning of the Pleistocene (~2.7 Ma). This major climate cooling and aridity maxima between 4.1-4.0 Ma is independently validated by a coeval sea-level drop (third order Za2 sequence boundary). This sea level drawdown is supported by enhanced coarse sedimentation and minima in riverine nutrient supply, showing paired vegetation and sea-level changes and thus a strong land-ocean relationship. This study also shows that long-term climatic trends were interrupted by orbital-scale cyclic climatic variability, with eccentricity, obliquity and precession acting as the main triggers controlling climate and environmental change in the area.

1. Introduction

The early Pliocene (Zanclean stage; between 5.3 and 3.6 Ma) is a very interesting period because it encompasses the so-called Pliocene climatic optimum (PCO) from 4.4 to 4 Ma, probably the warmest interval in this epoch with global average temperature ~ 4 °C higher than today (Brierley and Fedorov, 2010; Fedorov et al., 2013). Carbon dioxide reconstructions show higher-than-present values around 410 μatm (Bartoli et al., 2011) and a global sea-level about 25 m higher than present (Miller et al., 2005). Therefore, a great effort has been put into obtaining palaeoclimate records for the Pliocene, as it is recognized as the most recent example of prolonged global warmth in a higher-than-today CO_2 context in the geological past (Fedorov et al., 2013) and a very good analog for future climate change (Robinson et al., 2008).

Marine isotopic records suggest that a climate cooling took place from the warmer and more stable early Pliocene to the colder and more variable Pleistocene (Lisiecki and Raymo, 2005). This gradual cooling was probably due to a decrease in atmospheric carbon dioxide of about 100 parts per million (Bartoli et al., 2011). Even though the

Pliocene is thought to be a warmer period than today, a recent review by De Schepper et al. (2014) shows evidences of significant glaciation events in both northern and southern Hemispheres during this epoch. A progressive aridification in the Mediterranean area also happened during the Pliocene (Fauquette et al., 1998; Popescu et al., 2010; Jiménez-Moreno et al., 2013a), as well as the establishment of the Mediterranean-type seasonal precipitation rhythm (summer drought) at ~ 3.4 Ma (Suc, 1984; Suc and Popescu, 2005; Jiménez-Moreno et al., 2010). All these changes greatly affected past terrestrial environments in the Mediterranean area and vegetation experienced a decrease and disappearance of many thermophilous and hygrophilous species and the increase in xerophytes and Mediterranean adapted taxa (Suc, 1984; Popescu et al., 2010). Very few studies provide with information about how terrestrial western Mediterranean environments reacted to such long- and short-term climatic changes (Suc, 1984; Bertini, 2001; Combourieu-Nebout et al., 2004; Jiménez-Moreno et al., 2010; 2013a). Therefore, detailed pollen studies are needed to improve our knowledge about vegetation changes and the main forcings triggering cyclical vegetation changes during the early Pliocene in the Mediterranean area (i.e., Gauthier and Muñoz, 2009).

In the present study, we show a detailed and continuous record of pollen, percentage of sand and abundance of the benthic foraminifer *Bolivina spathulata* from a marine sedimentary record from the Guadalquivir Basin (SW Spain). This was done with the main goal of describing long-term paleoenvironmental and paleoclimate trends during the early Pliocene climatic optimum in the study area. This record shows that besides long-term trends, climate was also characterized by cyclical variability (i.e., orbital changes) that forced both terrestrial (e.g., vegetation changes of forested vs. open vegetation) and marine (sedimentation, organic matter fluxes, sea-level) environmental changes. The possible triggers of the observed orbital-scale variability are also discussed.

2. Geological setting

The study area is the western sector of the Guadalquivir Basin in SW Spain (Fig. 1A). This ENE-WSW-elongated foreland basin is limited to the north by the passive Iberian Massif and to the south by the active Betic Cordillera (Braga et al., 2002; González-Delgado et al., 2004). The Guadalquivir Basin has been linked to the isostatic subsidence produced by the loading of the Betic units on the south Iberian margin during the Neogene. By the earliest Tortonian, the Guadalquivir Basin was the Atlantic side of the North Betic Strait, connecting the Atlantic Ocean and the Mediterranean Sea (Martín et al., 2014; Braga et al., 2010). Afterwards, its paleogeography became an open and wide Atlantic bay (Martín el al., 2009), mostly in absence of fault tectonics (Fernàndez et al., 1998; Garcia-Castellanos et al., 2002), although subject to slow geodynamic vertical motions related to the mantle dynamics under the Betic cordillera (Garcia-Castellanos et al., 2002; Garcia-Castellanos & Villaseñor, 2011; Pérez-Asensio et al., 2018). During the Pliocene, the coastline steadily migrated westwards (Sierro et al., 1996) due to the axial sediment input together with the flexural isostatic response of the Betic-Guadalquivir-Hercynian massif system. Flexural basculation towards the south, in combination with the main sediment source being in the Betic cordillera, determined an axial (along-strike) fluvial drainage running along the northern boundary of the sedimentary basin (Garcia-Castellanos, 2002) as the Guadalquivir River does today. Sediments filling the Guadalquivir Basin are organized in several marine and continental units ranging from the Tortonian to the Holocene and the olistostromic deposits from the Betic Cordillera (Riaza and Martínez del Olmo, 1996; Sierro et al., 1990, 1996; González-Delgado et al., 2004; Salvany et al., 2011; Larrasoaña et al., 2014; Aguirre et al., 2015; Rodríguez-Ramírez et al., 2016).

Neogene sediments from the study area have been ascribed to eight marine and continental lithostratigraphic units (Civis et al., 1987; Salvany et al., 2011) (Fig. 1). The lowermost unit over the Iberian Massif basement is the Niebla formation (late Tortonian), which is composed of coastal carbonate-siliciclastic deposits (Civis et al., 1987; Baceta and Pendón, 1999). The second unit is the Gibraleón Formation (latest Tortonian-early Pliocene) and includes greenish-bluish clays with glauconitic silts at its base (Civis et al., 1987; Flores, 1987; Sierro et al., 1993; Pérez-Asensio et al., 2018). A Transitional Unit (late Messinian-early Pliocene) comprising transitional facies with alternating silts and sands is found over the Gibraleón Formation in central areas of the basin (De Torres, 1975; Mayoral and González, 1986–1987; Muñiz and Mayoral, 1996; Pérez-Asensio et al., 2018). The third unit, the Huelva Formation (early Pliocene), consists of silts and sands with a glauconitic layer at the base (Civis et al., 1987). The fourth unit is the sandy Bonares Formation (early Pliocene) (Mayoral and Pendón, 1986-87). Four continental units have been described above the marine units (Salvany et al., 2011). The Almonte Formation (Upper Pliocene-Lower Pleistocene) is the first continental unit, and is comprised of gravels and sands from proximal-alluvial deposits. Proximal sediments from this unit are the so-called High Alluvial Level (Pendón and Rodríguez-Vidal, 1986–1987; Salvany et al., 2011). The second continental unit is the Lebrija Formation (late Pliocene-late Pleistocene), which includes sands, gravels and clays from distal-alluvial deposits. The two last continental units (latest Pleistocene-Holocene) are the continental Abalario Formation and the continental-estuarine Marismas Formation. They consist of eolian sands and alluvial-estuarine clays, respectively.

3. Material and methods

The 276-m-long La Matilla (LM) core was drilled in the vicinity of Mazagón (Huelva) in the western Guadalquivir Basin (37º10'26.77''N, 6º43'27.14''W; 47 m altitude; Fig. 1). The LM core, currently curated at the Geological and Mining Institute of Spain (IGME) core repository, was drilled by IGME in 2006 using a rotary drilling rig with continuous core sampling. The core description, including lithostratigraphy, facies analysis and assignation of different units to the different formations outcropping in the lower Guadalquivir Basin area, was previously done in Pérez-Asensio et al. (2018).

The LM core chronology was developed from a combination of biostratigraphy and magnetostratigraphy (for a detailed explanation, see Pérez-Asensio et al., 2018; Fig. 2). Following the age model produced by these authors, the LM core contains a continuous early Pliocene sedimentary record comprised between 4.50 and 3.95 Ma (Pérez-Asensio et al., 2018; Fig. 2). The basinward migration of depositional facies in the Guadalquivir Basin explains why stratigraphic formations classically attributed to the Late Miocene in land sections (e.g., Gibraleón Formation) have an early Pliocene age at the location of LM core (Pérez-Asensio et al., 2018). Age estimates for the studied samples from the La Matilla core were assigned by assuming linear accumulation rates between the age tie points provided by the paleomagnetic boundaries (the tops of chrons C3n.2n, C3n.1r, and C3n.1n). For the lowermost part of the core (N1 polarity interval), the sedimentation rate of the R1 polarity interval (42.9 cm/ka) was extrapolated downward (Fig. 2). In the upper part of the core (R2 and an interval of uncertain polarity), the sedimentation rate of the R2 polarity interval (49.9 cm/ka) was extrapolated upward (Fig. 2). This resulted in an age of 3.95 Ma for the end of marine sedimentation (Fig. 2).

The percentage of sand content in the different facies along the 3 studied marine units (Fig. 2) was calculated every 3 m (83 samples) dividing the weight of the sand fraction (>63 µm) by the total sample weight (50 g) and multiplying by 100.

Samples (2 cm^3) for palynological analyses were taken roughly every 5 m throughout the core, with a total of 52 samples analyzed. The palynomorph extraction method followed a modified Faegri and Iversen (1989) methodology. Counting was performed at x400 and x1000 magnifications to a minimum pollen sum of 300 terrestrial pollen grains. Fossil pollen was compared with present-day relatives using published keys (e.g., Beug, 1961) and a modern pollen reference collection at the University of Granada (Spain). The raw counts were transformed to pollen percentages based on the terrestrial sum excluding *Pinus* - usually overrepresented in marine environments because of the advantage of bisaccate pollen for long-distance transport (Heusser, 1988; Jiménez-Moreno et al., 2005). The pollen zonation of the detailed pollen diagram was accomplished using CONISS (Grimm, 1987; Fig. 3). Arboreal Pollen (AP) abundance was calculated based on the total pollen sum with and without *Pinus*. Furthermore, pollen taxa were grouped, according to present-day ecological bases, into thermophilous (subtropical) trees. The thermophilous tree group includes Arecaeae, Taxodioideae, Rutaceae, Euphorbiaceae, *Cissus*, *Prosopis*, *Engelhardia* and Sapotaceae. An AP/arid ratio was calculated in order to discriminate between warm/humid (i.e., interglacial/interstadial phases) and cold/arid (i.e., glacial/stadial phases). As arid taxa, we included *Artemisia*, *Ephedra*, *Lygeum* and Asteraceae total (Cichorioideae and Asteroideae). Dinoflagellate cysts (dinocysts) occur with the pollen in the studied samples but at very low occurrences, which precluded their statistical study.

Principal Components Analysis (PCA) using PAST version 3.24 (Hammer et al., 2001) was run on the most abundant pollen taxa time series (Fig. 4). This was done to find hypothetical variables (components; i.e., environmental or climate parameters) accounting for as much as possible of the variance in the pollen data. A PCA correlation scatter diagram is shown in Fig. 4. This diagram shows to what degree the different taxa correlate with the principal component 1 (PC1) and 2 (PC2). PC1 data time series is represented in Figures 4B and 5.

A cyclostratigraphic analysis was performed on the *Quercus* and AP raw pollen percentages and PC1 pollen time series from the LM sedimentary sequence (Fig. 6). We used the software PAST (Hammer et al., 2001) with the program REDFIT (Schulz and Mudelsee, 2002) with the objective of characterizing the different periodicities present in the unevenly spaced raw pollen data.

A total of 83 samples of 50 g were analyzed for benthic foraminifera. At least 300 benthic foraminifera from the size fraction >125 μm were counted and identified. The relative abundances (%) of the benthic foraminifer *Bolivina spathulata* (Fig. 7) were obtained from transforming the raw counts of this species into percentages. Higher abundances of this shallow infaunal species were used as proxy for higher organic matter fluxes linked to riverine discharge (Duchemin et al., 2008; Schmiedl et al., 2010; Pérez-Asensio et al., 2014).

4. Results

4.1. Sand content

Sand content of the marine units of the LM sediment core shows an overall increasing trend towards the top of the core and varies from 0.2 (255 m; 4.44 Ma) to 93.4 % (48 m; 4.01 Ma) (Fig. 2). Very low sand % values (lower than 10%) characterize the core bottom, from 275 (4.49 Ma) to 150 m (4.21 Ma). Sand % increases in three cyclical increasing-decreasing cycles since then, with peaks of 14, 20 and 33% at 147 (4.21 Ma), 132 (4.18 Ma) and 114 m (4.14 Ma), respectively. Minimum values (<5%) are reached again between 102-96 m (4.12-4.10 Ma). An increase in sand % is observed later on, with a maximum of 68% at 81 m (4.07 Ma). Sand values decreased after this peak, and another minimum of ~20% is recorded at 78-75 m (4.07-4.06 Ma). A substantial increase is observed then with a peak of ~80% recorded at 60 m (4.03 Ma). A relative minimum of 58% is recorded at 57 m (4.02 Ma). Another increase-decrease cyclical oscillation is observed between 57 and 39 m (4.02-3.99 Ma), with a maximum in sand of 93% recorded at 48 m (4.01 Ma) and another drop in the sand values at 39 m (3.99 Ma). An increase in sand % with values around 70% characterize the record between 36-33 m (3.987-3.985 Ma).

4.2. Pollen analysis

Seventy-three different pollen taxa have been identified in the LM sedimentary record pollen spectra. The record shows diverse pollen taxa. However, many of the identified taxa occur in percentages lower than 1% and have not been plotted in Figure 3. These rare species include thermophilous (subtropical) plants such as Arecaceae, Taxodioideae, Rutaceae, Euphorbiaceae, *Cissus*, *Prosopis*, *Engelhardia* and Sapotaceae. Temperate tree species are also diversified, but many of them occur in very low percentages (i.e., *Acer*, *Castanea-Castanopsis* type, *Rhus*, *Pterocarya*, *Carya*, *Juglans*, *Corylus*, *Liquidambar*, *Distylium*, *Lonicera*, *Hedera* and *Ulmus*), except for *Quercus* (see below).

Overall, the LM core pollen record shows high abundances of non-arboreal pollen (NAP) (i.e., herbs and grasses), with average abundances around 75%. NAP pollen is dominated by Asteraceae Cichorioideae, Asteraceae Asteroideae, Poaceae and Amaranthaceae, and in smaller abundances, *Plantago*, Apiaceae, Cistaceae, *Ephedra*, *Artemisia* and Liliaceae. With respect to the AP, taxa are dominated by *Pinus* varying around average values of 26%. Less abundant trees are mostly dominated by evergreen and deciduous *Quercus*, *Olea*, Cupressaceae, *Cedrus* and *Cathaya*. Aquatics such as Cyperaceae also occur in this record but in low average abundances around 1%. We used variations in pollen species to objectively zone the pollen data using the program CONISS (Grimm, 1987), producing three pollen zones for the LM record (Fig. 3). The pollen results in these zones are described below:

Pollen zone LM-1 (267 – 250 m, 4.47 – 4.43 Ma) is characterized by high NAP percentage, with high abundance of Asteraceae Cichorioideae of around 40%, Poaceae around 22% and Asteraceae Asteroideae around 10%.

Pollen zone LM-2 (250 – 105 m, 4.43 – 4.12 Ma) features a significant decrease in NAP and the highest percentages of AP, which shows many cyclical oscillations and several peaks above 45%. This zone is then characterized by the highest occurrences in *Quercus* total (evergreen and deciduous) of 23% at the beginning of this zone at 216 m (~4.35 Ma). *Pinus* and *Quercus* total stay relatively abundant but show a decreasing trend throughout this zone. *Olea*, *Cathaya* and *Cedrus* occur in this zone with discrete occurrences.

Pollen zone LM-3 (105 – 30 m, 4.12 – 3.97 Ma) is characterized by the decrease in AP (notably in *Pinus* and *Quercus* but also in *Cathaya* and *Cedrus*) and the highest values of NAP of the LM record, with two maxima centered at ~100 and 50 m (4.1 and 4.0 Ma). *Olea* and Cupressaceae also increased and show maxima in this zone, featuring an increasing trend interrupted by two cyclical oscillations.

PCA analysis on a selection of most abundant pollen taxa from the LM record shows two main groups of distinctive taxa (Fig. 4A). PC1+ group, characterized by positive correlation to PC1, is made up of the most abundant tree taxa such as *Pinus*, *Quercus* (both evergreen and deciduous), *Cathaya*, *Cedrus* and the halophytic herb Amaranthaceae. PC1- group is characterized by negative correlation to PC1 and is dominated by non-arboreal species, such as Asteraceae Cichorioideae, Asteraceae Asteroideae, Poaceae, *Ephedra*, and Mediterranean-adapted tree species *Olea* and Cupressaceae. PCA analysis indicates that PC1 (probably a combination of temperature and precipitation, see below) is strong, explaining the 44.12% of the variance. Pollen data and CONISS cluster analysis agree with the PC1 (correlation of PC1 with AP: r=0.92; $p<0.01$; PC1 with *Quercus* total r=0.48; $p<0.01$) and pollen zones LM-1 and LM-3 are characterized by low abundances in the PC1+ pollen group and zone LM-2 is characterized by the highest values in the PC1+ (Fig. 4B).

4.3. Periodicity of pollen changes

Pollen data show a very clear cyclical pattern in the relative abundance of many taxa such as *Quercus* (Fig. 3). The PC1 is also characterized by cyclical oscillations, which covary with those observed in the raw *Quercus*, AP, thermophilous and AP/arid ratios (Figs. 4B, 5; see discussion below). Spectral analysis on the *Quercus* and AP pollen data and PC1 shows statistically significant (above the 80 and 90% confidence level) spectral peaks with periodicities between 80 - 67, 51 - 44, 37, 30 and 22-21 ka (Fig. 6).

4.4. Benthic foraminifer Bolivina spathulata

Relative abundance (%) of *Bolivina spathulata* changes considerably throughout the studied sediment core and varies from 0 to 50% (Fig. 7). The bottom part of the record between 273 – 240 m (4.49 – 4.41 Ma) is characterized by low values around 10%. An increase is observed then, reaching the maximum value of the record (~48%) at 213 m (4.35 Ma). A decreasing trend is observed since then, interrupted by cyclical variability, reaching several minima and the occasional absence of this species between 100 and the top of the record (since 4.12 Ma).

5. Discussion

5.1. Vegetation, benthic foraminifera and sedimentation as paleoenvironmental and paleoclimate proxies

Pollen analysis on Miocene and Pliocene marine sedimentary sequences from the Iberian Peninsula area have shown the highly sensitive response of pollen records to climate change, recording vegetation changes related to long-term and short-term orbital-scale climate variability (Jiménez-Moreno et al., 2007; 2010; 2013b). These previous studies show that the abundance of thermophilous forest species such as subtropical and temperate taxa can be used to track temperature changes through time. Hygrophilous species can also be used as proxies for precipitation, although sometimes it is difficult to separate the temperature vs. precipitation signals, for certain species require both high temperature and precipitation (or the opposite) to thrive. In this study we also used present-day thermophilous (i.e., subtropical) and temperate adapted species as proxies for temperature (Fig. 5). In this respect, *Quercus* (both evergreen and deciduous species) abundance has been shown to be an excellent proxy recording warm-humid vs. cold-arid (e.g., interglacials vs. glacials) paleoclimate phases in the southern Iberian Peninsula (Combourieu-Nebout et al 2002; Jiménez-Moreno et al., 2013b; Camuera et al., 2018, 2019). AP abundance can be used as a proxy for precipitation, for forested species require more water availability to grow than NAP taxa (Faegri and Iversen, 1987; Herzschuh, 2007). Here we added the arid indicators (*Artemisia*, *Ephedra* and Asteraceae total) to the forested humid/non-forested arid equation, calculating an AP/arid ratio as a better proxy for precipitation. The observed covariation between the PC1 with the above mentioned proxies for temperature and precipitation also indicate that increases in PC1 are related to warm/humid periods (Fig. 5). We are unsure about how to interpret the climatic inference of the herb Amarathaceae in this pollen record. Statistically it seems to be associated with the tree-dominated PC1+ group, however, in zone LM-02 it also shows a timid and progressive increasing trend, covarying at that time with the aridity proxies so it looks like it might be a mixed signal.

Bolivina spathulata abundance can be used as a proxy for organic matter fluxes related with high freshwater riverine input (Duchemin et al., 2008; Schmiedl et al., 2010). This species can tolerate low-oxygen conditions and prefer environments with supply of terrestrial degraded organic matter related to river runoff (Barmawidjaja et al., 1992; Stefanelli, 2004; Duchemin et al., 2008; Schmiedl et al., 2010) (Fig. 7). Previous studies showed high abundance of *B. spathulata* during interglacial-like periods, characterized by high riverine discharge bringing nutrients into the ocean (Pérez-Asensio et al., 2014).

Lithological changes (i.e., sand content) of the LM sedimentary core can be used as a proxy for relative sea-level oscillations controlling the proximity to coast of the studied site and thus the amount of coarse detritic input from the continent (Fig. 7).

5.2. Climate change recorded in the LM core during the early Pliocene

High abundances of NAP in the pollen spectra from LM indicate overall open vegetation environments and arid conditions during the early Pliocene in the studied area. The occurrence of herbaceous subdesertic taxa such as *Lygeum*, supports this interpretation. Occurrences of subtropical species also point to a warm subtropical climate. Climate was warmer than today, which is indicated by the higher occurrence of thermophilous taxa currently living in warmer areas of North Africa (Suc et al., 1995). This agrees with previous studies from the area for the early Pliocene, which show similar vegetation and climate estimations of mean annual temperatures around 21ºC and mean annual precipitation of ~400-600 mm (Andalucía G1 site; Jiménez-Moreno et al., 2010). A mosaic of different plant associations inherited from the Miocene and organized in altitudinal belts characterized the vegetation at that time. Subtropical evergreen-deciduous species lived at low elevations, an open mixed deciduous forest (mainly made up of conifers like *Pinus*, and several deciduous trees such as *Quercus*), occurred at higher altitude, and conifers such as *Cathaya* and *Cedrus* grew at higher elevations on the surrounding mountains.

Significant long-term changes in climate are observed during the early Pliocene between 4.5 and 3.9 Ma in the SW Guadalquivir Basin region. This is deduced by changes in the terrestrial vegetation that parallel marine benthic fauna and sedimentary variations in the LM core (Fig. 7). The beginning of the studied record (including LM-1 pollen zone) at around 4.45 Ma begins with overall cold and arid climate conditions. Relatively low organic matter fluxes (low *B. spathulata* abundances) is also recorded at that time, indicating low riverine runoff, which further support aridity at that time. This interpretation agrees with climate inferences obtained from previous palynological studies showing a cooling event at ~4.5 Ma, in the marine pollen record from the Andalucía G1 site (Suc et al., 1995), located offshore of S Iberia and 300 km SE of LM, and in the marine pollen record from the Garraf 1 site in NE Iberian Peninsula (Suc and Cravatte, 1982). Globally, this time period corresponds with relatively low sea level, right after the Za1 minimum sea-level sequence boundary (Handerbol et al., 1998), which would agree with cold conditions during a period of eccentricity minima (Laskar et al., 2004; Fig. 8).

Rapid warming and enhanced humid conditions occurred after ~4.37 Ma, and warmest and wettest conditions in the vicinity of the LM record were reached at around 4.35 Ma. (Figs. 7 and 8). This is deduced by the highest occurrences in *Quercus* total, thermophilous and AP/arid ratios of the LM record (Fig. 5). Conifers requiring relatively high humidity such as *Cedrus* and *Cathaya* reached their maxima around that time (Fig. 3), supporting highest humidity. Highest *B. spathulata* abundances are also recorded at 4.35 Ma in the LM record (Fig. 7), indicating highest fluvial runoff supplying continental degraded organic matter. Warmest conditions at that time are supported by low global ice volume deduced by global isotopic composition of benthic foraminifera (perhaps the CN3 isotopic event; Lisiecki and Raymo, 2005), and high insolation and eccentricity, coinciding with the early Pliocene climatic optimum and high global sea level (Fig. 8). Warmest conditions at this time are also recorded regionally in other pollen records from the Mediterranean area such as the marine sedimentary sequences of Cap d'Adge 1 and Pichegu (Suc et al., 2018).

Overall, warm and humid conditions prevailed after this warmest maximum during pollen zone LM-02 until 4.13 Ma. However, a progressive climate cooling and aridity trend interrupted by cyclic climatic variability also characterized the LM record (Fig. 8). This is deduced by the progressive decrease in abundance of *Quercus*, thermophilous, high AP/arid ratios and PC1 (Fig. 5). Riverine nutrient supply deduced from the LM record covaried with the vegetation also featuring a significant decreasing trend at that time (Fig. 7). This indicates a progressive decrease in riverine runoff with a decaying supply in degraded organic matter from the continent into the marine environment, which agrees with the increasing trend in aridity. This environmental change observed in the LM record could be related with the cooling trend and increase in global ice volume deduced by the increase in the global isotopic $\delta^{18}O$ stack record (Lisiecki and Raymo, 2005), perhaps related with a decrease in eccentricity and its modulating effect in summer insolation (Laskar et al., 2004) (Fig. 8). A progressive increase in sand content occurred in the LM record between 4.21 and 4.14 Ma (Fig. 7). This could be due to a sea-level glacio-eustatic lowering due to the progressive cooling, generating enhanced influence of coarse terrestrial sedimentation due to closeness to coast. West-southwestward progradation of terrigenous depositional systems along the axial part of the Guadalquivir Basin and also from North-east (passive border), filling up the basin, would account for the important increase in coarser detritics and sedimentary rates in a context of sea-level lowering in this area, as deduced by previous studies (Sierro et al., 1996; Pérez-Asensio et al., 2018; Jiménez-Moreno et al., 2013b). This gradual filling could have been accelerated in a context of eustatic sea level lowering with the subsequent decrease in accommodation space in the Guadalquivir basin.

This cooling trend ended with significant glaciation-like cold and arid events that affected the terrestrial environments in the study area at ~ 4.1 and 4.0 Ma (LM-03 pollen zone) (Fig. 8). Coldest/driest conditions at this time are deduced by lowest *Quercus*, AP/arid and PC1 values (Fig. 5). Similar very low percentages (<5%) in *Quercus* forest were reached during the last two glaciations (ca. 20 and 140 ka) in the southern Iberian Peninsula (Camuera et al., 2019), supporting our climatic interpretations. Related with this major climate cooling and aridity maxima, was enhanced coarse sedimentation and minima in organic matter fluxes to the seafloor due to low riverine discharge, showing paired vegetation and sea-level changes and a strong land-ocean relationship (Fig. 7). Coldest/driest conditions of the LM record could be related to significant glaciation events recorded in the marine isotopic records of benthic $\delta^{18}O$ Gi24-20 (Lisiecki and Raymo, 2005) and minima in eccentricity (Fig. 8). The glacio-eustatic sea-level drop associated with this especially cold glacial period was recorded globally as a third order

(Za2) sequence boundary (Fig. 8; Handerbol et al., 1998), affecting our study site with a significant regression, increasing its proximity to the coast and enhancing coarse sedimentation (Fig. 7). The evidences of glacial-like conditions between 4.1-4.0 Ma in the LM area are supported by a recent review about climate variability during the Pliocene by De Schepper et al. (2014), who show evidences of a significant glaciation event in both northern and southern Hemispheres at around 4.0 Ma. This glacial-like climatic event occurred during the early Pliocene climatic optimum, a period known by very little terrestrial evidence of glaciation, and indicates that major glaciation-like cooling occurred before the intensification of northern hemisphere glaciation at the beginning of the Pleistocene (~2.7 Ma; Lisiecki and Raymo, 2005). This cooling trend and associated glacio-eustatic sea-level lowering might have contributed to the final continentalization of the study area that occurred at about 30 m core depth in the LM sediment core (Almonte and Abalario Fm.; Fig. 1). A previously mentioned cause that could have triggered enhanced cooling and glaciation at this time in the Northern Hemisphere is the constriction of the Indonesian Seaway between 4-3 Ma, generating a weakening of the Atlantic Meridional Overturning Circulation, which regulates climate in the area (Karas et al., 2017).

An increase in climate seasonality (i.e., summer drought) seems to have affected the terrestrial environments in the study area since 4.12 Ma and related with the above mentioned significant glacial event. This is deduced by the increasing trend in *Olea*, a typical Mediterranean and summer-drought-adapted sclerophyllous taxon, from 4.12 Ma towards the top of the LM record at 3.97 Ma (Fig. 7). Previous studies noticed a major reduction in subtropical taxa and an increase in sclerophyllous vegetation during the late Pliocene at around 3.4-3.2 Ma, which they interpreted as the effect on the vegetation of the onset of the Mediterranean-type seasonal precipitation rhythm in the Mediterranean area (Suc, 1984; Suc and Popescu, 2005). Our pollen data from the LM record indicate that this change towards a more seasonal Mediterranean-like climate could have started earlier, at around 4 Ma ago. However, more data from additional sites in the area are necessary to confirm this, as the *Olea* pollen change is small (from 0 to 4%; Fig. 7). Anyway, the climate change to a colder, drier and more seasonal climate at this time had considerable effects on Pliocene environments and vegetation, reducing tropical species worldwide, and triggering the disappearance of forests and the spread of more open and xeric landscapes (see regional syntheses in Jiménez-Moreno et al., 2010; Biltekin et al., 2015; Fauquette et al., 2018).

5.3. Climate variability during the early Pliocene

Previous paleoclimatic studies concluded that initial assumption of persistent global warmth and stable Pliocene climate conditions were not substantiated (Prescott et al., 2014), and temperatures were as variable as those during the late Pleistocene (Lawrence et al., 2009). In this study, we show that long-term scale trends in climate in the early Pliocene LM record are interrupted by shorter-orbital-scale cyclical climatic changes, deduced by the alternation between thermophilous-temperate forest (i.e., AP) and herbs (i.e., NAP), most-likely representing warm/humid-cold/arid climatic cycles, respectively (see explanation above). Different scale cyclicities can be observed visually in the pollen abundances (Fig. 5) and statistically through spectral analysis of the *Quercus*, AP and PC1 data time-series (Fig. 6). Two main and statistically significant vegetation and climate cyclicities can be noticed in the three studied proxies, with periodicities around 51-37 and 22-21 ka, which could be related with obliquity (~41 ka) and precession (~21 ka) orbital cycles, respectively (Laskar et al., 2004). We are unsure about the significance of the later 22-21 ka cycle, since the average sample resolution in the study record is 9.4 ka, perhaps insufficient to statistically support this cycle. However, the occurrence of this cycle is supported by previous studies suggesting that precession induced climatic oscillations in rainfall in this area generated cyclical variations in the input of freshwater and sedimentation into the Guadalquivir Basin and Gulf of Cadiz during the early Pliocene (Ledesma, 2000; Sierro et al., 2000). Two other obtained statistically significant cyclicities are ~80-67 and 30 ka, which are more difficult to interpret but could be related to a mixed signal of different orbital-scale cycles (eccentricity, obliquity and precession; Berger, 1977). Lisiecki and Raymo (2005) also obtained a similar spectral peak at 29 ka on the last 860 ka of the LR04 benthic $\delta^{18}O$ stack, which they interpreted as a nonlinear climate response. We are unassertive about why the 100-ka eccentricity cycle is not showing up in the spectral analyses, as visually it seems to be characterizing the main variability of the environmental and vegetation changes (see *Quercus* data filtered to 100-ka and correlations to short-term eccentricity in Fig. 8). Long-term eccentricity (~400 ka) cycles are not obtained in the spectral analysis either as the record is too short to register several of these cycles but seems to be the one controlling long-term environmental and climatic evolution in this area (long-term minima in *Quercus* or AP/arid ratios in pollen zones LM-01 and LM-03, at 4.5-4.4 and 4.1-4.0 Ma; Fig. 8). The 400-ka cycle has previously been reported to be one of the main controls of cyclical marine sedimentation in the Guadalquivir and Gulf of Cadiz area (Ledesma, 2000; Sierro et al. 2000). The sea-level drop recorded at ~4.0 Ma, coinciding with the 3rd order sequence boundary Za2 (Hardenbol et al., 1998), is simultaneous with an eccentricity minimum related to the long-term eccentricity cycle and thus is interpreted here to have a glacio-eustatic origin. This orbital-scale variability seems to be reciprocated in the proxy for continental organic matter fluxes to the seafloor (*B. spathulata* abundance), showing minima during cold events (Fig. 7) and pointing to simultaneous variations and fast responses in the terrestrial and marine environments due to same orbital-scale climate oscillations. Overall, the presence of orbital changes in the studied LM record support the age model of Pérez-Asensio et al. (2018) even for its uppermost part, were magnetobiostratigraphic tie points could not be retrieved due to a change in paleoenvironmental conditions and a loss in paleomagnetic quality.

This study reveals the strong influence of the eccentricity and obliquity orbital-scale climatic changes on the environment in the study area. Long- and short-term eccentricity are one of the most significant orbital-scale cycles controlling climate and environmental changes recorded in late Miocene and Pliocene sedimentary sequences (Braga and Martin, 1996; Shackleton and Crowhurst, 1997; Ledesma, 2000; Vidal et al., 2002; Pérez-Asensio et al., 2012, 2013; Jiménez-Moreno et al., 2013a, b; van den Berg et al., 2015, 2018). In the mid-latitude Mediterranean area, cyclical changes in the vegetation are mostly forced by precession (Kloosterboer-van Hoeve, 2006; Tzedakis, 2007). Nevertheless, obliquity seems to have also played an important role in shaping the vegetation during the Pliocene and Pleistocene period (Popescu, 2001; Popescu et al., 2010; Suc et al., 2010; Joannin et al., 2007, 2008; Jiménez-Moreno et al., 2013a; this study). This indicates a high-latitude impact on the climate from the Mediterranean area through variations in seasonal contrast, mainly controlling temperature changes (Tuenter et al., 2003; Suc et al., 2010).

Conclusions

The detailed multiproxy study on an early Pliocene marine sedimentary record from SW Spain shows:

1. Warmest and wettest conditions during the 4.5-3.9 Ma period occurred in this area at ~4.35 Ma. Highest organic matter fluxes to the seafloor related to riverine discharges are also recorded at this time, supporting high fluvial runoff supplying continental degraded organic matter. This agrees with warmest conditions shown by low global ice volume deduced by global isotopic composition of benthic foraminifera, and high insolation and eccentricity, coinciding with the early Pliocene climatic optimum and high global sea level.
2. Vegetation and riverine nutrient supply proxies show a subsequent cooling and drying trend after the warmest maximum until ~4.13 Ma. This environmental change could be related with the cooling trend and increase in global ice volume, perhaps caused by a decrease in eccentricity and its modulating effect on summer insolation. A progressive increase in sand content in the LM record between 4.21 and 4.14 Ma could also indicate a glacio-eustatic lowering of the sea-level. West-southwestward progradation of terrigenous depositional systems along the axial part of the Guadalquivir Basin and important detrital inputs from the Iberian Massif prograding towards the center, filling up the basin, would account for the important increase in coarser detritics in a context of sea-level lowering in this area.
3. This cooling trend ended with significant glaciation-like cold and arid events affecting the study area between ~4.1 and 4.0 Ma. Related with this major climate cooling and aridity maxima was enhanced coarse sedimentation and minima in riverine nutrient supply to the ocean, showing paired vegetation

and sea-level changes and a strong land-ocean relationship. Coldest/driest conditions of the LM record could be related to significant glaciation events (Gi24-20) recorded in the marine isotopic records and minima in eccentricity. The glacio-eustatic sea-level drop associated with this glaciation affected our study site with a significant regression, increasing its proximity to the coast and enhancing coarse sedimentation and was recorded globally as a third order (Za2) sequence boundary.

4. Our study shows that terrestrial and marine environments were forced by long- and short-term eccentricity, obliquity and perhaps precession orbital cycles, shaping vegetation, fluvial organic matter fluxes to the seafloor and sedimentary changes in SW Iberia.

Acknowledgements

This study was supported by the research projects CGL2012-30875 (GUADALTYC), CGL2013-47038-R, CGL-2017-85415-R and CGL2014-59516 (MITE) of the Ministerio de Economía y Competitividad of Spain, project P11-RNM-7332 from the Junta de Andalucía, and the Research Groups RNM-190 of the Junta de Andalucía and GRC Geociències Marines (2017 SGR 315) of the Generalitat de Catalunya.

References

Aguirre, J., Braga, J.C., Martín, J.M., Puga-Bernabéu, Á., Pérez-Asensio, J.N., Sánchez-Almazo, I.M., and Génio, L., 2015. An enigmatic kilometer-scale concentration of small mytilids (late Miocene, Guadalquivir Basin, S Spain). Palaeogeography, Palaeoclimatology, Palaeoecology 436, 199–213.

Baceta, J.I., Pendón, J.G., 1999. Estratigrafía y arquitectura de facies de la Formación Niebla, Neógeno superior, sector occidental de la Cuenca del Guadalquivir. Revista de la Sociedad Geológica de España 12, 419–438.

Barmawidjaja, D.M., Jorissen, F.J., Puskaric, S., van der Zwaan, G.J., 1992. Microhabitat selection by benthic foraminifera in the northern Adriatic Sea. Journal of Foraminiferal Research 22, 297–317.

Bartoli, G., Hönisch, B., Zeebe, R.E., 2011. Atmospheric CO_2 decline during the Pliocene intensification of Northern Hemisphere glaciations, Paleoceanography, 26, PA4213.

Berger, A.L., 1977. Support for the astronomical theory of climatic change. Nature 269, 44–45.

Bertini, A., 2001. Pliocene climatic cycles and altitudinal forest development from 2.7 Ma in the Northern Apennines (Italy): evidence from the pollen record of the Stirone section (−5.1 to −2.2 Ma). Geobios 34, 253–265.

Beug, H.-J., 1961. Leitfaden der Pollenbestimmung für Mitteleuropa und angrenzende Gebiete, Fisch. Stuttg., 61.

Bitelkin, D., Popescu, S.-M., Suc, J.-P., Quézel, P., Yavuz, N., Jiménez-Moreno, G., Safra, A., Namik Cagatay, M., 2015. Anatolia: a plant refuge area during the last 23 Million years according to pollen records from Turkey. Review of Palaeobotany and Palynology 215, 1-22.

Braga, J.C., Martín, J.M., 1996. Geometries of reef advance in response to relative sea-level changes in a Messinian (uppermost Miocene) fringing reef (Cariatiz reef, Sorbas Basin, SE Spain). Sedimentary Geology 107, 61–81.

Braga, J.C., Martín, J.M., Aguirre, J., 2002. Tertiary. Southern Spain. In: Gibbons, W., Moreno, T. (Eds.), The Geology of Spain. The Geological Society, London, pp. 320–327.

Braga, J.C., Martín, J.M., Aguirre, J., Baird, C.D., Grunnaleite, I., Jensen, N.B., Puga-Bernabéu, A., Saelen, G., Talbot, M.R., 2010. Middle-Miocene (Serravallian) temperate carbonates in a seaway connecting the Atlantic Ocean and the Mediterranean Sea (North Betic Strait, S Spain). Sedimentary Geology 225, 19–33.

Brierley, C., Fedorov, A., 2010. Relative importance of meridional and zonal sea surface temperature gradients for the onset of the ice ages and Pliocene-Pleistocene climate evolution. Paleoceanography 25, PA2214.

Camuera, J., Jiménez-Moreno, G., Ramos-Román, M.J., García-Alix, A., Toney, J.L., Anderson, R.S., Jiménez-Espejo, F.J., Kaufman, D., Bright, J., Webster, C., Yanes, Y., Carrión, J.S., Ohkouchi, N., Suga, H., Yamame, M., Yokoyama, Y., Martínez-Ruiz, F., 2018. Orbital-scale environmental and climatic changes recorded in a new ~ 200,000-year-long multiproxy sedimentary record from Padul, southern Iberian Peninsula. Quaternary Science Reviews 198, 91-114.

Camuera, J., Jiménez-Moreno, G., Ramos-Román, M.J., García-Alix, A., Toney, J.L., Anderson, R.S., Jiménez-Espejo, F., Bright, J., Webster, C., Yanes, Y., Carrión, J.S., 2019. Vegetation and climate changes during the last two glacial-interglacial cycles in the western Mediterranean: A new long pollen record from Padul (southern Iberian Peninsula). Quaternary Science Reviews 205, 86-105.

Civis, J., Sierro, F.J., González-Delgado, J.A., Flores, J.A., Andrés, I., de Porta, J., Valle, M.F., 1987. El Neógeno marino de la provincia de Huelva: Antecedentes y definición de las unidades litoestratigráficas. In: Civis, J. (Ed.), Paleontología del Neógeno de Huelva. Ediciones Universidad de Salamanca, Salamanca, pp. 9–21.

Combourieu-Nebout, N., Turon, J.L., Zahn, R., Capotondi, L., Londeix, L., Pahnke, K., 2002. Enhanced aridity and atmospheric high-pressure stability over the western Mediterranean during the North Atlantic cold events of the past 50 k.y. Geology 30 (10), 863-866.

Combourieu-Nebout, N., Foucault, A., Mélières, F., 2004. Vegetation markers of palaeoclimate cyclical changes in the Pliocene of Punta Piccola (Sicily, Italy). Palaeogeography, Palaeoclimatology, Palaeoecology 214, 55–66.

De Schepper, S., Gibbard, P.L., Salzmann, U., Ehlers, J., 2014. A global synthesis of the marine and terrestrial evidence for glaciation during the Pliocene Epoch. Earth-Science Reviews 135, 83–102.

De Torres, T., 1975. Mapa Geológico Nacional: Instituto Geológico y Minero de España Sheet Number 984, scale 1:50,000, 14 pp.

Duchemin, G., Jorissen, F.J., Le Loc'h, F., Andrieux-Loyer, F., Hily, C., Thouzeau, G., 2008. Seasonal variability of living benthic foraminifera from the outer continental shelf of the Bay of Biscay. Journal of Sea Research 59, 297–319.

Faegri, K., Iversen, J., 1989. Textbook of Pollen Analysis. New York: Wiley.

Fauquette, S., Guiot, J., Suc, J.-P., 1998. A method for climatic reconstruction of the Mediterranean Pliocene using pollen data. Palaeogeography, Palaeoclimatology, Palaeoecology 144, 183–201.

Fauquette, S., Suc, J.-P., Médail, F., Muller, S.D., Jiménez-Moreno, G., Bertini, A., Martinetto, E., Popescu, S.-M., Zheng, Z., de Beaulieu, J.-L., 2018. The Alps: A geological, climatic, and human perspective on vegetation history and modern plant diversity. In: Hoorn, C., Perrigo, A., Antonelli, A., (Eds.), Mountains, Climate, and Biodiversity, First Edition. Wiley-Blackwell, pp. 413-428.

Fedorov, A.V., Brierley, C.M., Lawrence, K.T., Liu, Z., Dekens, P.S., Ravelo, A.C., 2013. Patterns and mechanisms of early Pliocene warmth. Nature 496, 43-49.

Fernàndez, M., Beràstegui, X., Puig, C., García-Castellanos, D., Jurado, M.J., Torné, M., Banks, C., 1998. Geophysical and geological constraints on the evolution of the Guadalquivir foreland basin, Spain. In: Mascle, A., Puigdefabregas, C., Luterbacher, H. & Fernandez, M. (eds.). Cenozoic Foreland Basins of Western Europe. Geological Society of London Special Publications, 134, 29-48.

Flores, J.A., 1987. El nanoplancton calcáreo en la formación «Arcillas de Gibraleón»: Síntesis bioestratigráfica y paleoecológica. In: Civis, J. (Ed.), Paleontología del Neógeno de Huelva. Ediciones Universidad de Salamanca, Salamanca, Spain, pp. 65–68.

Garcia-Castellanos, D., 2002. Interplay between lithospheric flexure and river transport in foreland basins. Basin Research 14(2), 89-104.

Garcia-Castellanos, D., Fernàndez, M., Torné, M., 2002. Modelling the evolution of the Guadalquivir foreland basin (South Spain). Tectonics 21(3),

Garcia-Castellanos, D., Villaseñor, A., 2011. Messinian salinity crisis regulated by competing tectonics and erosion at the Gibraltar Arc. Nature, 480, 359-363.

Gauthier, A., Munoz, A., 2009. Seasonal sedimentation in the Pliocene Villaroya Lake (N Spain) inferred from pollen analysis. Sedimentary Geology 222 (1-2), 111-123.

González-Delgado, J.A., Civis, J., Dabrio, C.J., Goy, J.L., Ledesma, S., Pais, J., Sierro, F.J., Zazo, C., 2004. Cuenca del Guadalquivir. In: Vera, J.A. (Ed.), Geología de España. SGE-IGME, Madrid, pp. 543–550.

Grimm, E.C., 1987. CONISS: a Fortran 77 program for stratigraphically constrained cluster analysis by the method of incremental sum of squares. Computers and Geosciences 13, 13–35.

Hammer, O., Harper, D.A.T., Ryan, P., 2001. Past: paleontological statistics software package for education and data analysis. Palaeontologia Electronica 4 (1) (art. 4, 9 pp.).

Hardenbol, J., Thierry, J., Farley,M.B., Jaquin, T., de Graciansky, P., Vail, P.R., 1998. Mesozoic and Cenozoic sequence chronostratigraphic framework of European basins - chart 2: Cenozoic sequence chronostratigraphy. In: de Graciansky, P., Hardenbol, J., Jaquin, T., Vail, P.R. (Eds.), Mesozoic and cenozoic sequence stratigraphy of european basins: SEPM Special Publication, 60.

Herzschuh, U., 2007. Reliability of pollen ratios for environmental reconstructions on the Tibetan Plateau. Journal of Biogeography 34, 1265–1273.

Heusser, L., 1988. Pollen distribution in marine sediments on the continental margin of northern California. Mar. Geol. 80, 131– 147.

Hilgen, F.J., Lourens, J.A., Van Dam, L.J., Beu, A.G., Boyes, A.F., Cooper, R.A., Krijgsman, W., Ogg, J.G., Piller, W.E., Wilson, D.S., 2012. The Neogene Period. In: Gradstein, F.M., Ogg, J.G., Schmitz, M.D., Ogg, G.M., (Eds.), The Geologic Time Scale. Boston Elsevier, pp. 923-978.

Jiménez-Moreno, G., Rodríguez-Tovar, F.-J., Pardo-Igúzquiza, E., Fauquette, S., Suc, J.-P., Müller, P., 2005. High-resolution palynological analysis in late Early–Middle Miocene core from the Pannonian Basin, Hungary: climatic changes, astronomical forcing and eustatic fluctuations in the Central Paratethys. Palaeogeography, Palaeoclimatology, Palaeoecology 216 (1–2), 73–97.

Jiménez-Moreno, G., Abdul-Aziz, H., Rodríguez-Tovar, F. J., Pardo-Igúzquiza, E., Suc, J.-P., 2007. Palynological evidence for astronomical forcing in Early-Middle Miocene lacustrine deposits from Rubielos de Mora Basin (NE Spain). Palaeogeography, Palaeoclimatology, Palaeoecology 252, 601-616.

Jiménez-Moreno, G., Suc, J.-P., Fauquette, S., 2010. Miocene to Pliocene vegetation reconstruction and climate estimates in the Iberian Peninsula from pollen data. Review of Palaeobotany and Palynology 162, 403–415.

Jiménez-Moreno, G., Burjachs, F., Expósito, I., Oms, O., Carrancho, A., Villalain, J.J., van der Made, J., Agustí, J., Campeny, G., Gómez de Soler, B., 2013a. Late Pliocene vegetation and orbital-scale climate changes from the western Mediterranean area. Global and Planetary Change 108, 15-28.

Jiménez-Moreno, G., Pérez-Asensio, J.N., Larrasoaña, J.C., Aguirre, J., Civis, J., Rivas-Carballo, M.R., Valle-Hernández, M.F., González-Delgado, J.A., 2013b. Vegetation, sea-level and climate changes during the Messinian salinity crisis. Geological Society of America Bulletin 125, 432-444

Joannin, S., Quillévéré, F., Suc, J.-P., Lécuyer, C., Martineau, F., 2007. Early Pleistocene climate changes in the central Mediterranean region as inferred from integrated pollen and planktonic foraminiferal stable isotope analyses. Quaternary Research 67, 364–374.

Joannin, S., Ciaranfi, N., Stefanelli, S., 2008. Vegetation changes during the late early Pleistocene at Montalbano Jonico (Province of Matera, southern Italy) based on pollen analysis. Palaeogeography, Palaeoclimatology, Palaeoecology 270, 92–101.

Karas, C., Nürnberg, D., Bahr, A., Groeneveld, J., Herrle, J.O., Tiedemann, R., deMenocal, P.B., 2017. Pliocene oceanic seaways and global climate. Scientific Reports 7:39842.

Kloosterboer-van Hoeve, M.L., Steenbrink, J., Visscher, H., Brinkhuis, H., 2006. Millennial-scale climatic cycles in the Early Pliocene pollen record of Ptolemais, northern Greece. Palaeogeography, Palaeoclimatology, Palaeoecology 229, 321–334.

Larrasoaña, J.C., Liu, Q., Hu, P., Roberts, A.P., Mata, P., Civis, J., Sierro, F.J., Pérez-Asensio, J.N., 2014. Paleomagnetic and paleoenvironmental implications of magnetofossil occurrences in late Miocene marine sediments from the Guadalquivir Basin, SW Spain. Frontiers in Microbiology, 5, Article 71.

Laskar, J., Robutel, P., Joutel, F., Gastineau, M., Correia, A.C.M., Levrard, B., 2004. A long-term numerical solution for the insolation quantities of the Earth. Astronomy & Astrophysics 428, 261–285.

Lawrence, K. T., Herbert, T.D., Brown, C.M., Raymo, M.E., Haywood, A.M., 2009. High-amplitude variations in North Atlantic sea surface temperature during the early Pliocene warm period, Paleoceanography, 24, PA2218.

Ledesma, S., 2000. Astrobiocronología y estratigrafía de alta resolución del Neógeno de la Cuenca del Guadalquivir-Golfo de Cádiz. PhD dissertation, University of Salamanca, Spain.

Lisiecki, L. E., Raymo, M.E., 2005. A Pliocene-Pleistocene stack of 57 globally distributed benthic $\delta^{18}O$ records. Paleoceanography 20, PA1003.

Martín, J.M., Braga, J.C., Aguirre, J., Puga-Bernabéu, A., 2009. History and evolution of the North-Betic Strait (Prebetic Zone, Betic Cordillera): a narrow, early

Tortonian, tidal-dominated, Atlantic–Mediterranean marine passage. Sedimentary Geology 216, 80–90.

Martín, J.M., Puga-Bernabéu, A., Aguirre, J., and Braga, J.C., 2014. Miocene Atlantic-Mediterranean seaways in the Betic Cordillera (southern Spain). Revista de la Sociedad Geológica de España 27, 175–186.

Mayoral, E., González, I., 1986–1987. Contribución al estudio de las facies de tránsito Mioceno-Plioceno en el sector noroccidental de la Cuenca del Guadalquivir (Valencina de la Concepción, Sevilla). Acta Geológica Hispánica 21–22, 177–184.

Mayoral, E., Pendón, J.G. 1986-87. Icnofacies y sedimentación en zona costera. Plioceno superior (?), litoral de Huelva. Acta Geologica Hispanica 21-22: 507-513.

Miller, K.G., Kominz, M.A., Browning, J.V., Wright, J.D., Mountain, G.S., Katz, M.E., Sugarman, P.J., Cramer, B.S., Christie-Blick, N., Pekar, S.F., 2005. The Phanerozoic record of global sea-level change. Science 310, 1293–1298.

Muñiz, F., Mayoral, E., 1996. Características paleoambientales de las <<facies de tránsito>> (Plioceno inferior) en el sector N.O. de la Cuenca del Gualdalquivir (Albaida del Aljarafe, Sevilla, España). Geogaceta 20, 207–208.

Pendón, J.G., and Rodríguez-Vidal, J., 1986–1987. Caracteres sedimentológicos y geomorfológicos del Alto Nivel Aluvial cuaternario en el litoral de Huelva. Acta Geológica Hispánica 21–22, 107–111.

Pérez-Asensio, J.N., Aguirre, J., Schmiedl, G., Civis, J., 2012. Impact of restriction of the Atlantic–Mediterranean gateway on the Mediterranean Outflow Water and eastern Atlantic circulation during the Messinian. Paleoceanography 27, PA3222. http://dx.doi.org/10.1029/2012PA002309.

Pérez-Asensio, J.N., Aguirre, J., Jimenez-Moreno, G., Schmiedl, G., and Civis, J., 2013. Glacioeustatic control on the origin and cessation of the Messinian salinity crisis. Global and Planetary Change 111, 1–8.

Pérez-Asensio, J.N., Aguirre, J., Schmiedl, G., Civis, J., 2014. Messinian productivity changes in the northeastern Atlantic and their relationship to the closure of the Atlantic–Mediterranean gateway: Implications for Neogene palaeoclimate and palaeoceanography. Journal of the Geological Society [London] 171, 389–400.

Pérez-Asensio, J.N., Larrasoaña, J.C., Samankassou, E., Sierro, F.J., Garcia-Castellanos, D., Jiménez-Moreno, G., Salazar, A., Salvany, J.M., Ledesma, S., Mata, M.P., Civis, J., Mediavilla, C., 2018. Magnetobiochronology of Lower Pliocene marine sediments from the lower Guadalquivir Basin: Insights into the tectonic evolution of the Strait of Gibraltar área. *GSA Bulletin* 130 (11-12), 1791-1808.

Popescu, S.-M., 2001. Repetitive changes in Early Pliocene vegetation revealed by high-resolution pollen analysis: revised cyclostratigraphy of southwestern Romania. Review of Palaeobotany and Palynology 120 (3–4), 181–202.

Popescu, S.M., Biltekin, D., Winter, H., Suc, J.-P., Melinte-Dobrinescu, M.C., Klotz, S., Rabineau, M., Combourieu-Nebout, N., Clauzon, G., Deaconu, F., 2010. Pliocene and Lower Pleistocene vegetation and climate changes at the European scale: long pollen records and climatostratigraphy. Quaternary International 219, 152–167.

Prescott, C.L., Haywood, A.M., Dolan, A.M., Hunter, S.J., Pope, J.O., Pickering, S.J., 2014. Assessing orbitally-forced interglacial climate variability during the mid-Pliocene Warm Period. Earth and Planetary Science Letters 400, 261-271.

Riaza, C., Martínez del Olmo, W., 1996. Depositional model of the Guadalquivir-Gulf of Cádiz Tertiary basin. In: Friend, P., Dabrio, C.J. (Eds.), Tertiary basins of Spain. Cambridge University Press, Cambridge, pp. 330–338.

Robinson, M., Dowsett, H.J., Chandler, M.A., 2008. Pliocene role in assessing future climate impacts. Eos Transactions American Geophysical Union 89, 501-502.

Rodríguez-Ramírez, A., Villarías-Robles, J.J.R., Pérez-Asensio, J.N., Santos, A., Morales, J.A., Celestino-Pérez, S., León, Á., Santos-Arévalo, F.J., 2016. Geomorphological record of extreme wave events during Roman times in the Guadalquivir estuary (Gulf of Cadiz, SW Spain): an archaeological and paleogeographical approach. Geomorphology 261, 103–118.

Salvany, J.M., Larrasoaña, J.C., Mediavilla, C., and Rebollo, A., 2011. Chronology and tectono-sedimentary evolution of the Upper Pliocene to Quaternary deposits of the lower Guadalquivir Basin, SW Spain. Sedimentary Geology 241, 22–39.

Schmiedl, G., Kuhnt, T., Ehrmann, W., Emeis, K.-C., Hamann, Y., Kotthoff, U., Dulski, P., Pross, J., 2010. Climatic forcing of eastern Mediterranean deep-water and benthic ecosystems during the past 22 000 years. Quaternary Science Reviews 29, 3006–3020.

Schulz, M., Mudelse, A., 2002. REDFIT: estimating red-noise spectra directly from unevenly spaced paleoclimatic time series. Computers & Geosciences 28, 421–426.

Shackleton, N.J., Crowhurst, S., 1997. Sediment fluxes based on orbitally tuned time scale 5 Ma to 14 Ma, Site 926. In: Shackleton, N.J., Curry, W.B., Richter, C., Bralower, T.J., et al., (Eds.). Proceedings of the Ocean Drilling Program, Scientific Results, Volume 154: College Station, Texas, Ocean Drilling Program, pp. 69–82.

Sierro, F.J., Gonzalez-Delgado, J.A., Dabrio, C., Flores, J.A., and Civis, J., 1990. The Neogene of the Guadalquivir basin (SW of Spain). In: Agustí, J., Domènech, R., Julià, R., and Martinell, J., (eds.), Paleontologia i Evolució Memòria Especial 2: Iberian Neogene Basins. Sabadell, Spain, Diputació de Barcelona, pp. 209–250.

Sierro, F.J., Flores, J.A., Civis, J., González-Delgado, J.A., Francés, G., 1993. Late Miocene globorotaliid event-stratigraphy and biogeography in the NE-Atlantic and Mediterranean. Marine Micropaleontology 21, 143–168.

Sierro, F.J., González Delgado, A., Dabrio, C.J., Flores, A., Civis, J., 1996. Late Neogene depositional sequences in the foreland basin of Guadalquivir (SW Spain). In: Friend, P.F., and Dabrio, C.J., (eds.), Tertiary Basins of Spain. Cambridge, UK, Cambridge University Press, pp. 339–345.

Sierro, F.J., Ledesma, S., Flores, J.A., Torrescusa, S., Martínez del Olmo, W., 2000. Sonic and gamma-ray astrochronology: Cycle to cycle calibration of Atlantic climatic records to Mediterranean sapropels and astronomical oscillations. Geology 28, 695-698.

Stefanelli, S., 2004. Cyclic changes in oxygenation based on foraminiferal microhabitats: Early-Middle Pleistocene, Lucania Basin (southern Italy). Journal of Micropalaeontology 23, 81–95.

Suc, J.-P., Cravatte, J., 1982. Etude palynologique du Pliocène de Catalogne (nord-est de l'Espagne). Paléobiologie Continentale 13 (1), 1–31.

Suc, J.-P., 1984. Origin and evolution of the Mediterranean vegetation and climate in Europe. Nature 307, 429–432.

Suc, J.-P., Popescu, S.-M., 2005. Pollen records and climatic cycles in the Mediterranean region since 2.7 Ma. In: Head, M.J., Gibbard, P.L. (Eds.), Early–Middle Pleistocene Transitions, the Land–Ocean Evidence: Geological Society, London Special Publications, vol. 247, pp. 147–158.

Suc, J.-P., Diniz, F., Leroy, S., Poumot, C., Bertini, A., Dupont, L., Clet, M., Bessais, E., Zheng, Z., Fauquette, S., Ferrier, J., 1995. Zanclean (Brunssumian) to early Piacenzian (early–middle Reuverian) climate from 4 to 54° north latitude (West Africa, West Europe and West Mediterranean areas). Mededelingen - Rijks Geologische Dienst 52, 43–56.

Suc, J.-P., Combourieu-Nebout, N., Seret, G., Klotz, S., Popescu, S.-M., Gautier, F., Clauzon, G., Westgate, J., Sandhu, A.S., 2010. The Crotone series: a synthesis and new data. Quaternary International 219, 121–133.

Suc, J.-P., Popescu, S.-M., Fauquette, S., Bessedik, M., Jiménez-Moreno, G., Bachiri Taoufiq, N., Zheng, Z., Médail, F., Klotz, S., 2018. Reconstruction of Mediterranean flora, vegetation and climate for the last 23 million years based on an extensive pollen dataset. Ecologia Mediterranea 44 (2), 53-85.

Tuenter, E., Weber, S.L., Hilgen, F.J., Lourens, L.J., 2003. The response of the African summer monsoon to remote and local forcing due to precession and obliquity. Global and Planetary Change 36, 219–235.

Tzedakis, P.C., 2007. Seven ambiguities in the Mediterranean palaeoenvironmental narrative. Quaternary Science Reviews 26, 2042–2066.

Van den Berg, B.C.J., Sierro, F.J., Hilgen, F.J., Flecker, R., Larrasoaña, J.C., Krijgsman, W., Flores, J.A., Mata, M.P., Martín, E.B., Civis, J., González-Delgado, J.A., 2015. Astronomical tuning for the upper Messinian Spanish Atlantic margin: disentangling basin evolution, climate cyclicity and MOW. Global and Planetary Change 135, 89–103.

Van den Berg, B.C.J., Sierro, F.J., Hilgen, F.J., Flecker, R., Larrasoaña, J.C., Krijgsman, W., Flores, J.A., Mata, M.P., 2018. Imprint of Messinian Salinity Crisis events on the Spanish Atlantic margin. Newsletters on Stratigratigraphy 51, 93–115.

Vidal, L., Bickert, T., Wefer, G., Röhl, U., 2002. Late Miocene stable isotope stratigraphy of SE Atlantic ODP Site 1085: Relation to Messinian events. Marine Geology 180, 71–85.

Figure captions

Figure 1. (A) Simplified geological map of the study area and location of La Matilla (LM) sedimentary core. The regional cross section in B is also indicated. (B) A NW-SE cross section of the lower Guadalquivir Basin showing the main lithostratigraphic units and the LM core location. Modified from Pérez-Asensio et al. (2018).

Figure 2. The LM core lithology, sand content, variations in inclination of the characteristic remanent magnetization (ChRM) based on quality types 1 and 2 data and the associated pattern of polarity intervals identified, and location of biostratigraphic events recognized by planktonic foraminifera (modified from Pérez-Asensio et al., 2018). On the bottom right is the age-depth model and sedimentary rates (cm/k.y.) for the LM record (modified after Pérez-Asensio et al., 2018). Gray shadings and dashed lines indicate the interpreted correlation to the GTS2012 time scale (Hilgen et al., 2012). FO—first occurrence (lowest occurrence); LO—last occurrence (highest occurrence); LcO—last common occurrence (highest common occurrence); G.—*Globorotalia*.

Figure 3. Detailed pollen diagram of the early Pliocene LM core in depth (m) and age (Ma). Only species with percentages higher than 1% are shown. Arboreal pollen (AP) percentages are also plotted. Green and yellow indicate the trees and herbs, respectively. Shading in some pollen species is the exaggeration of their abundance x5. Aquatic Cyperaceae is in blue. On the right is a cluster analysis (Grimm, 1987) of the pollen results and pollen zones, Climatic inferences (with color shading, red indicating warm/humid, blue cold/dry) are shown in the pollen zones.

Figure 4. Principal Component Analysis (PCA) from the LM pollen data. (A) PCA scatter diagram with the most significant (abundant) pollen taxa. PCA (PC1+ and PC1-) groups are shown. The analysis was carried out using PAST (Hammer et al., 2001). (B) Obtained PC1 plot and AP (%) from LM record. Note the visual covariation with each other. Pollen zones are shown on the right with climatic inferences (with color shading, red indicating warm/humid, blue cold/dry).

Figure 5. Comparison of the pollen paleoclimatic proxies obtained from the early Pliocene LM record. From bottom to top: percentages of thermophilous taxa, percentages of *Quercus*, AP/arid ratios, and PC1. The pollen zones and climatic inferences (with color shading, red indicating warm/humid, blue cold/dry) are shown. Note the covariation of all proxies shown by dashed lines.

Figure 6. Spectral analysis of the most significant climatic pollen proxies from the early Pliocene LM record: *Quercus*, AP and PC1. Confidence levels are shown in orange (80% confidence level) and green (90% confidence level). Significant periodicities (above the 80 and 90% confidence level) are shown with numbers (all in ka). The spectral analysis

was done using the software PAST (Hammer et al., 2001). In pink shading are frequencies of orbital-scale eccentricity, obliquity and precession cycles.

Figure 7. Comparison of paleoclimatic, riverine nutrient supply and sedimentation (proximity to coast) proxies for the 4.5-3.9 Ma interval from LM record. From bottom to top are abundances (%) of: *Bolivina spathulata*, *Quercus*, *Olea* and sand content. Blue shading indicates cold/dry periods. Note the covariation of the proxies shown by dashed lines. Blue dashed line highlight the significant cooling/drying at ~4.12 Ma (see text for explanation).

Figure 8. Comparison of paleoclimatic pollen proxies from the LM record with global paleoclimatic records of the early Pliocene 4.5-3.9 Ma interval. From bottom to top: raw *Quercus* abundance (%) and filtered 100-ka component of the *Quercus* abundance from LM, PC1 from LM, LR04 benthic $\delta^{18}O$ record showing major isotopic events (Lisiecki and Raymo, 2005), orbital eccentricity (Laskar et al., 2004), summer insolation at 65ºN (Laskar et al., 2004) and global sea-level cycles of Hardenbol et al. (1998) with sequence boundaries Za1 and Za2. Blue shading indicates cold/dry periods. Dashed lines point to correlations between the LM record and global paleoclimatic and glacio-eustatic records: in blue are events corresponding to long-term eccentricity minima, in black are events corresponding to 100-ka eccentricity cycles and in orange are correlations to obliquity cycles (see text for explanation).

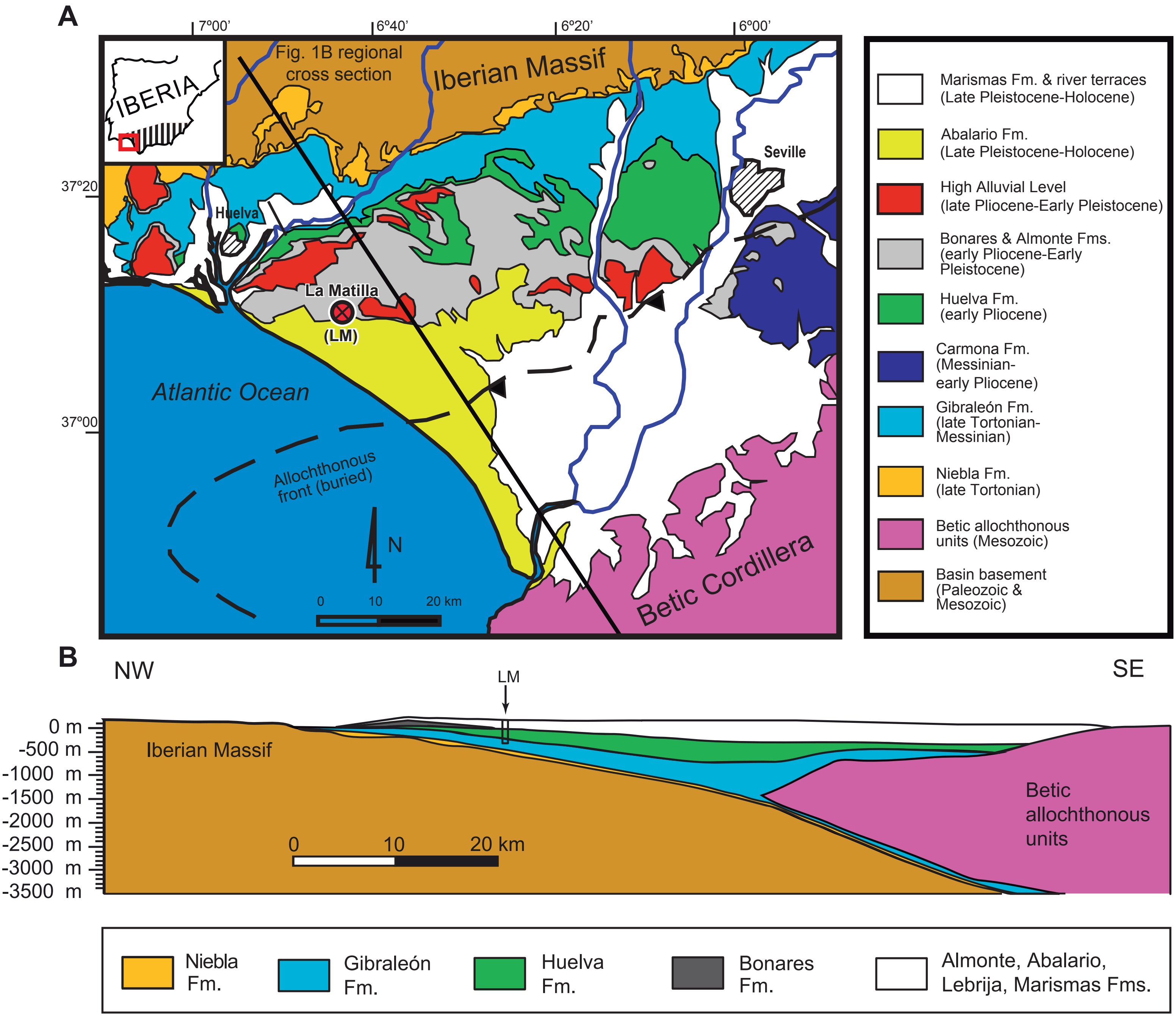
A
7°00'
6°40'
6°20'
6°00'
37°20
37°00
IBERIA
Fig. 1B regional cross section
Iberian Massif
Huelva
Seville
La Matilla
(LM)
Atlantic Ocean
Allochthonous front (buried)
N
0
10
20 km
Betic Cordillera
Marismas Fm. & river terraces (Late Pleistocene-Holocene)
Abalario Fm. (Late Pleistocene-Holocene)
High Alluvial Level (late Pliocene-Early Pleistocene)
Bonares & Almonte Fms. (early Pliocene-Early Pleistocene)
Huelva Fm. (early Pliocene)
Carmona Fm. (Messinian-early Pliocene)
Gibraleón Fm. (late Tortonian-Messinian)
Niebla Fm. (late Tortonian)
Betic allochthonous units (Mesozoic)
Basin basement (Paleozoic & Mesozoic)
B
NW
SE
LM
0 m
-500 m
-1000 m
-1500 m
-2000 m
-2500 m
-3000 m
-3500 m
Iberian Massif
Betic allochthonous units
0
10
20 km
Niebla Fm.
Gibraleón Fm.
Huelva Fm.
Bonares Fm.
Almonte, Abalario, Lebrija, Marismas Fms.

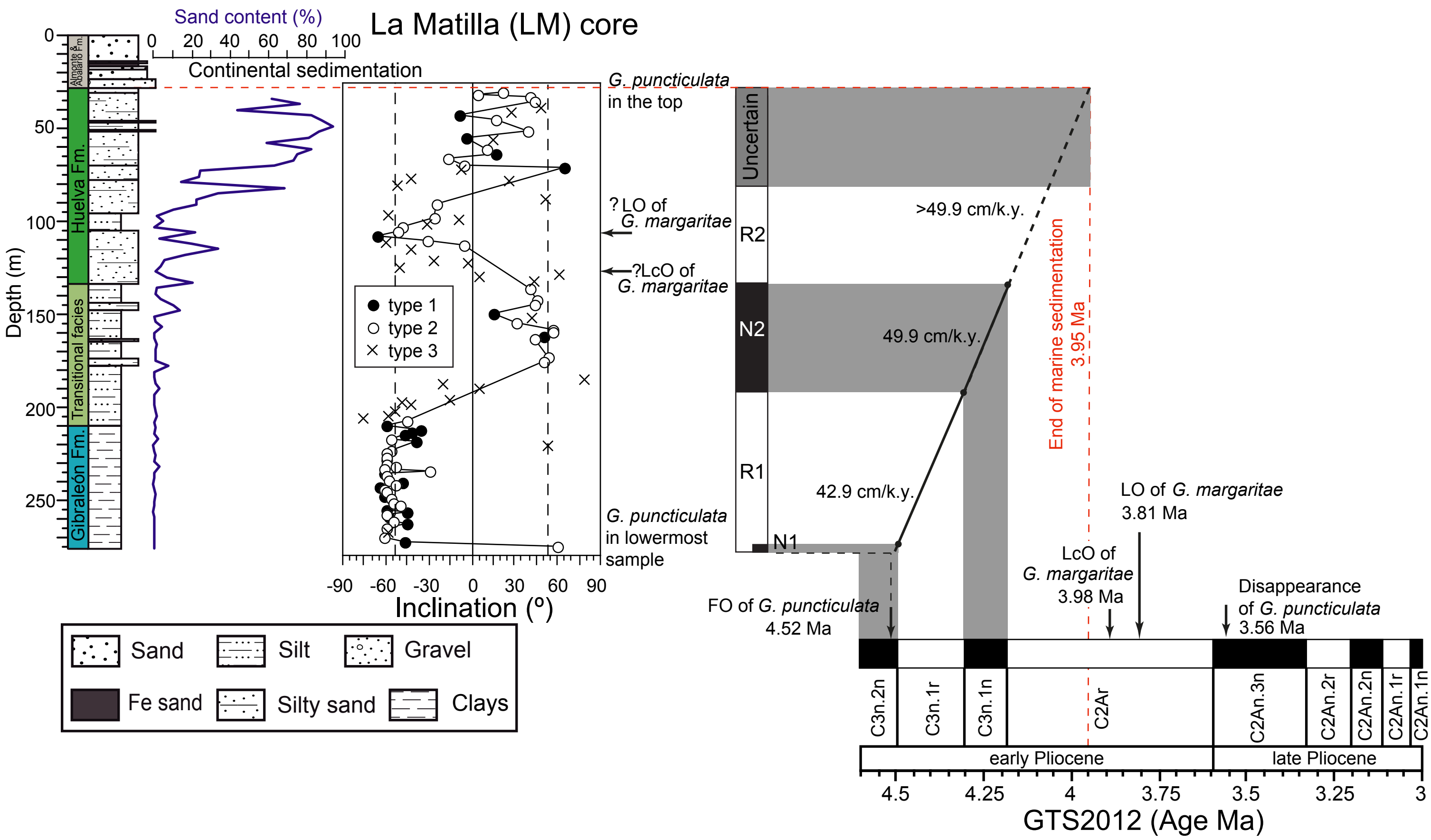

La Matilla (LM) core
Sand content (%)
0 20 40 60 80 100
Continental sedimentation
Depth (m)
0
50
100
150
200
250
Huelva Fm.
Transitional facies
Gibraleón Fm.
G. puncticulata in the top
?LO of G. margaritae
?LcO of G. margaritae
G. puncticulata in lowermost sample
type 1
type 2
type 3
-90 -60 -30 0 30 60 90
Inclination (º)
Sand
Silt
Gravel
Fe sand
Silty sand
Clays
Uncertain
R2
N2
R1
N1
>49.9 cm/k.y.
49.9 cm/k.y.
42.9 cm/k.y.
End of marine sedimentation 3.95 Ma
LO of G. margaritae 3.81 Ma
LcO of G. margaritae 3.98 Ma
FO of G. puncticulata 4.52 Ma
Disappearance of G. puncticulata 3.56 Ma
C3n.2n
C3n.1r
C3n.1n
C2Ar
C2An.3n
C2An.2r
C2An.2n
C2An.1r
C2An.1n
early Pliocene
late Pliocene
4.5
4.25
4
3.75
3.5
3.25
3
GTS2012 (Age Ma)

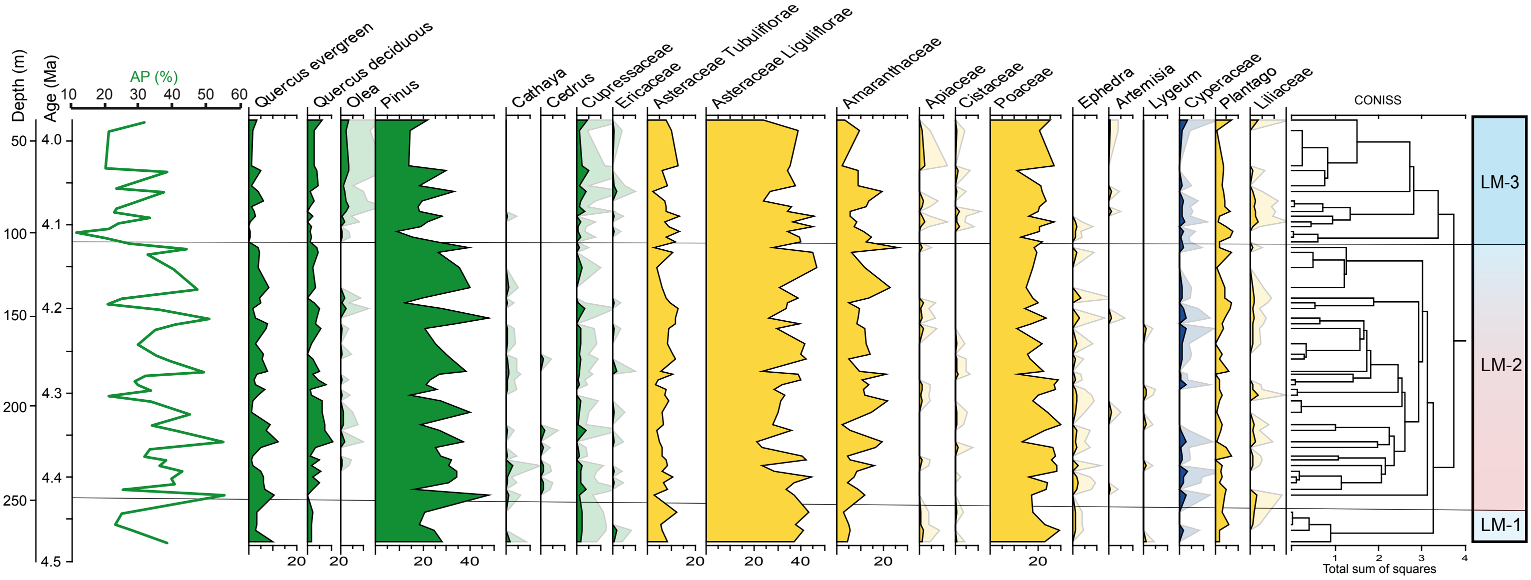
Depth (m)
Age (Ma)
AP (%)
Quercus evergreen
Quercus deciduous
Olea
Pinus
Cathaya
Cedrus
Cupressaceae
Ericaceae
Asteraceae Tubuliflorae
Asteraceae Liguliflorae
Amaranthaceae
Apiaceae
Cistaceae
Poaceae
Ephedra
Artemisia
Lygeum
Cyperaceae
Plantago
Liliaceae
CONISS
Total sum of squares
LM-3
LM-2
LM-1

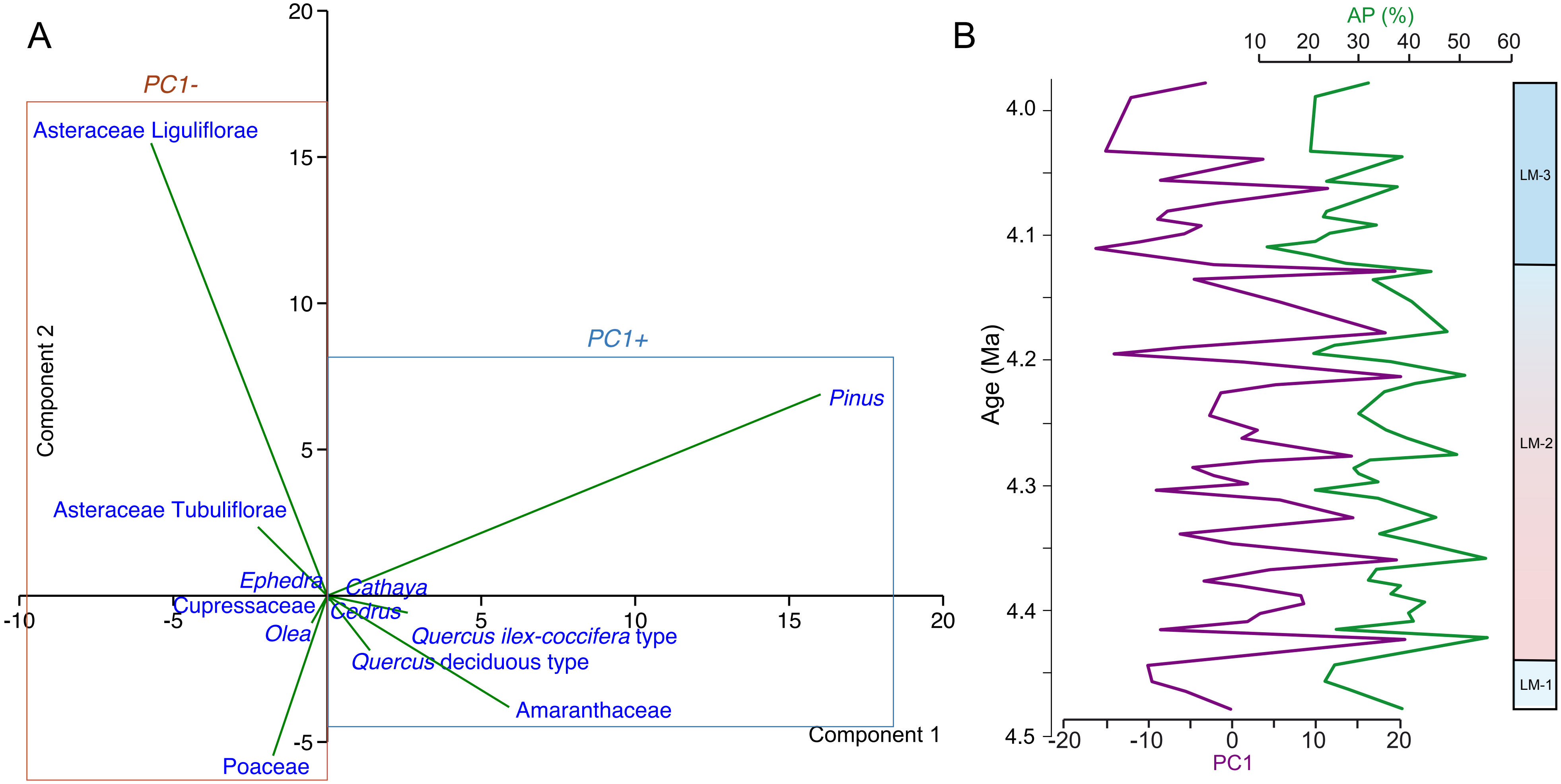

A
PC1-
PC1+
Asteraceae Liguliflorae
Asteraceae Tubuliflorae
Ephedra
Cupressaceae
Olea
Poaceae
Cathaya
Cedrus
Quercus ilex-coccifera type
Quercus deciduous type
Amaranthaceae
Pinus
Component 1
Component 2
B
AP (%)
Age (Ma)
PC1
LM-3
LM-2
LM-1

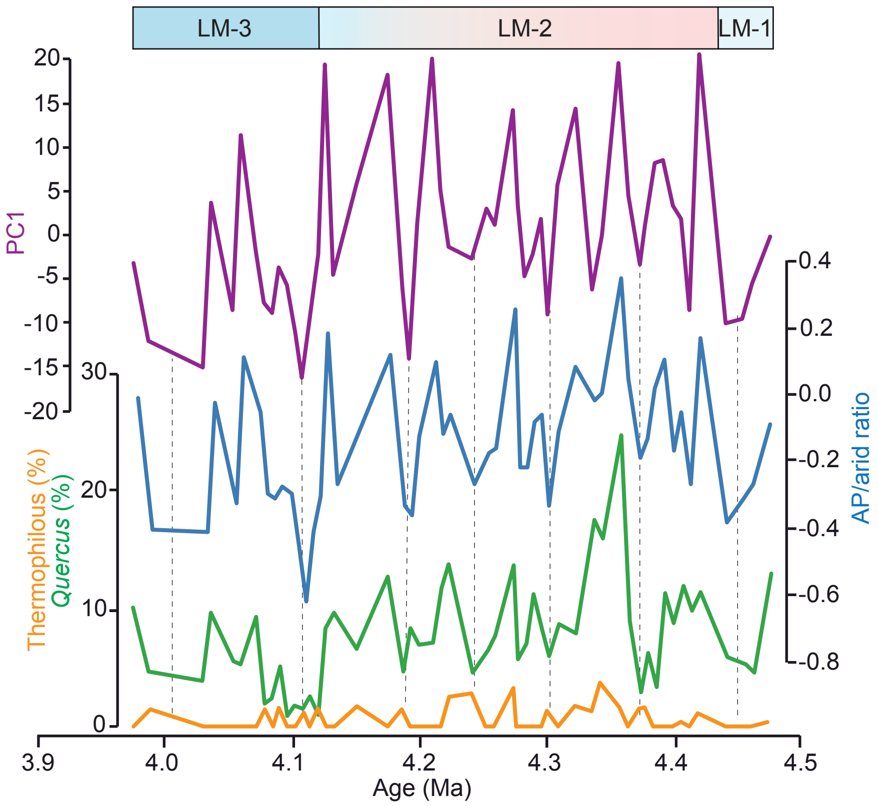

LM-3
LM-2
LM-1
PC1
20
15
10
5
0
-5
-10
-15
-20
Thermophilous (%)
Quercus (%)
30
20
10
0
0.4
0.2
0.0
-0.2
-0.4
-0.6
-0.8
AP/arid ratio
3.9
4.0
4.1
4.2
4.3
4.4
4.5
Age (Ma)

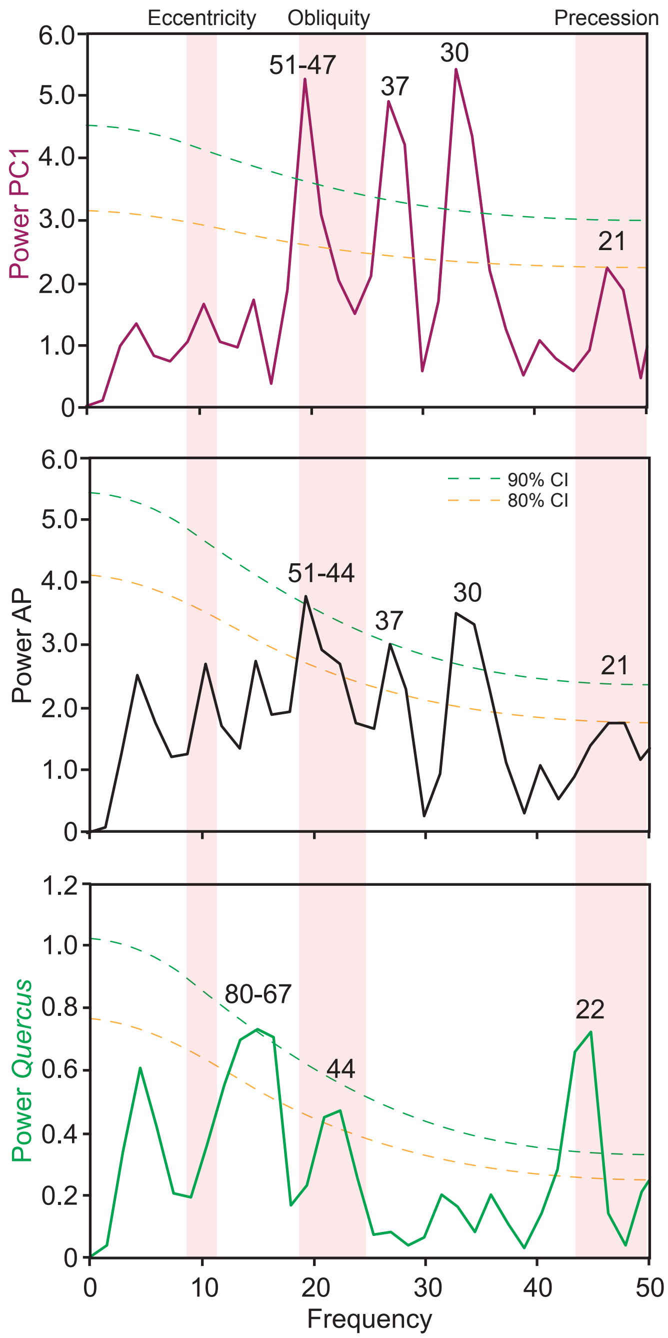

Eccentricity
Obliquity
Precession
Power PC1
51-47
37
30
21
Power AP
90% CI
80% CI
51-44
37
30
21
Power *Quercus*
80-67
44
22
Frequency

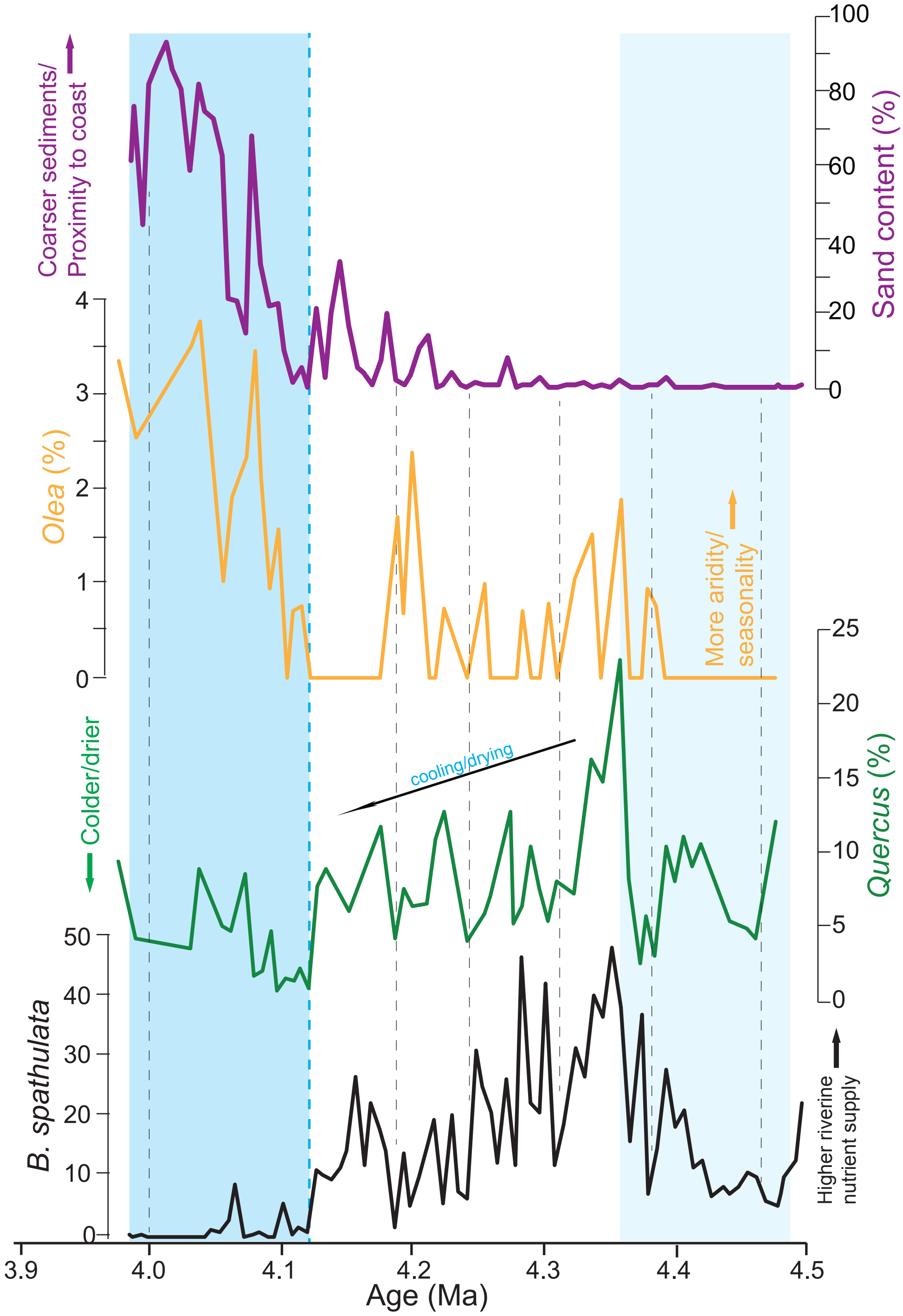

Coarser sediments/
Proximity to coast
Sand content (%)
100
80
60
40
20
0
Olea (%)
4
3
2
1
0
More aridity/
seasonality
cooling/drying
Colder/drier
Quercus (%)
25
20
15
10
5
0
B. spathulata
50
40
30
20
10
0
Higher riverine
nutrient supply
3.9
4.0
4.1
4.2
4.3
4.4
4.5
Age (Ma)

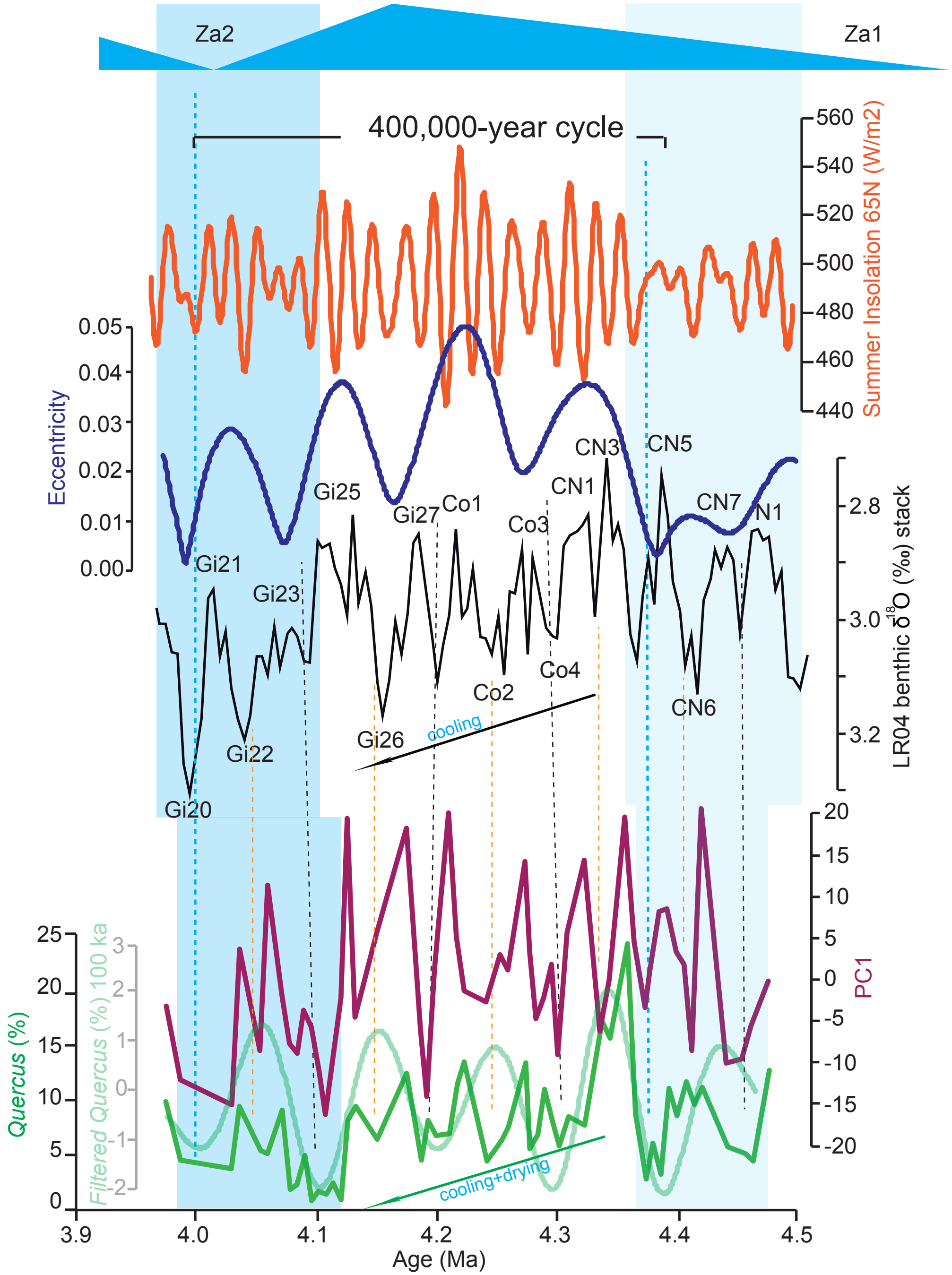
Za2
Za1
400,000-year cycle
Summer Insolation 65N (W/m2)
560
540
520
500
480
460
440
Eccentricity
0.05
0.04
0.03
0.02
0.01
0.00
LR04 benthic δ18O (‰) stack
2.8
3.0
3.2
Gi20
Gi21
Gi22
Gi23
Gi25
Gi26
Gi27
Co1
Co2
Co3
Co4
CN1
CN3
CN5
CN6
CN7
N1
cooling
PC1
20
15
10
5
0
-5
-10
-15
-20
Quercus (%)
25
20
15
10
5
0
Filtered Quercus (%) 100 ka
3
2
1
0
-1
-2
cooling+drying
3.9
4.0
4.1
4.2
4.3
4.4
4.5
Age (Ma)